Trends in
Biochemical Sciences

CellPress
OPEN ACCESS

Review

Unraveling the relationship between PET surfaces and their hydrolases

Marie Sofie Møller[1,*], Anton Bleckert[2], Anna Jäckering[2], and Birgit Strodel[2,3,*]

Plastics, especially polyethylene terephthalate (PET), are vital in modern life, with global production exceeding 400 million tons annually. This extensive use has led to significant plastic waste pollution, highlighting the need for effective recycling strategies. PET, one of the most recycled plastics, is a prime candidate for degradation into its original monomers through engineered PET hydrolases – enzymes with industrial potential. While previous engineering efforts have mainly focused on enhancing thermostability and catalytic efficiency, the crucial aspect of enzyme adsorption to PET surfaces has received less attention. This review specifically addresses the mechanisms of enzyme adsorption, detailing relevant experimental methods and simulation techniques while emphasizing the potential for engineering more effective PET hydrolases.

Highlights

The existence of polyethylene terephthalate (PET) hydrolases is striking, given that PET is a synthetic polymer and enzymes evolved for natural substrates.

To enhance the applicability of PET hydrolases in industrial settings, targeted enzyme reengineering is essential.

Strategies for improving PET hydrolases include increasing thermostability, accelerating catalytic reactions, and optimizing binding to PET substrates.

According to the Sabatier principle, achieving optimal binding strength between PET and PET hydrolases is crucial for effective catalysis.

A range of biochemical and biophysical techniques is available to enhance our understanding of PET hydrolase adsorption to PET, paving the way for advanced enzyme design.

Discovery and potential of PET hydrolases

The existence of enzymes capable of degrading **PET** (see Glossary), a synthetic anthropogenic polymer not found in nature, is remarkable. While enzymes have evolved to effectively target natural substrates, the presence of these enzymes that can degrade PET is surprising at first glance. However, upon closer examination, one finds that there are hydrolysable synthetic polymers like PET that share structural similarities, such as ester bonds, with natural polyesters like cutin, which are substrates for hydrolases. *Thermobifida fusca* cutinase (TfC) was the first PET-degrading enzyme discovered, as described in 2005 [1].

Since then, a number of **PET hydrolases** have been identified and advanced [2], including the leaf compost cutinase (LCC) and polyester hydrolase I (PES-H1, also known as PHL7) which were both derived from compost metagenome libraries in 2014 [3] and 2022 [4], respectively. LCC shows high activity against PET and exhibits cutinase-like properties, enabling the enzyme to break down polymer structures effectively. Building on this natural enzyme, the French company CARBIOS utilized the ICCG variant of LCC (F243I/D238C/S283C/Y127G) [5], enabling them to successfully launch the first enzymatic PET recycling demonstration plant in 2021 with plans to open a larger facility with a recycling capacity of 130 tons per day in 2025 (https://www.carbios.com/en/enzymatic-recycling/). Although PES-H1 is somewhat less active than LCC [6], it is of industrial interest, as well, as it demonstrates a broader substrate specificity that could be enhanced further through a two-enzyme system, similar to that employed by *Ideonella sakaiensis* 201-F6. This bacterium can effectively metabolize PET using the enzymes *Is*PETase and MHETase, which facilitate the complete degradation of PET into bis(2-hydroxyethyl) terephthalate (BHET) and mono(2-hydroxyethyl) terephthalate (MHET), ultimately producing the monomers terephthalic acid (TPA) and ethylene glycol (EG) [7].

Table 1 summarizes key wild-type (WT) and mutant PET hydrolases, detailing their enzymatic characteristics on both amorphous and crystalline PET substrates, along with the temperatures at which these parameters were measured. It highlights how enzyme performance varies with

[1]Applied Molecular Enzyme Chemistry, Department of Biotechnology and Biomedicine, Technical University of Denmark, DK-2800, Kgs. Lyngby, Denmark
[2]Institute of Biological Information Processing (IBI-7: Structural Biochemistry), Forschungszentrum Jülich, Jülich, Germany
[3]Institute of Theoretical and Computational Chemistry, Heinrich Heine University Düsseldorf, Düsseldorf, Germany

*Correspondence:
msmo@dtu.dk (M.S. Møller) and
b.strodel@fz-juelich.de (B. Strodel).

temperature and PET substrate crystallinity, with higher temperatures generally improving activity. Additionally, many values remain unestablished, underscoring the need for a more comprehensive understanding of enzymatic PET hydrolysis. To address this, Arnal *et al.* developed a standardized protocol for larger-scale studies, applying it to four PET hydrolases [16]. Their findings identified that FAST-PETase and HotPETase are unsuitable for large-scale applications due to low depolymerization rates, while PES-H1 L92F/Q94Y (PES-H1^{FY}) could be a promising candidate with 80% depolymerization upon further enzyme evolution. LCC^{ICCG} excelled, achieving 98% PET conversion to TPA and EG in 24 h, and they improved its economic viability by reducing enzyme usage by a factor of 3 and lowering the reaction temperature from 72°C to 68°C. Nonetheless, further optimization is crucial for enhancing the catalytic efficiency and environmental impact of enzymatic PET hydrolysis, as current life cycle assessments show that enzymatic PET recycling still lags behind virgin PET production in most categories [17]. Therefore, we will first examine the individual steps of the catalytic cycle, which present several opportunities for enzyme improvement, before focusing on the initial step: the adsorption of PET hydrolases onto the PET material.

The catalytic cycle and potential intervention points for engineering PET hydrolases

PET degradation by PET hydrolases can be considered as **heterogeneous catalysis**, where the catalyst is in a different phase (here solution) than the substrate (here solid). Consequently, the catalytic cycle involves the following steps (Figure 1). (i) Adsorption: the PET hydrolase must first come into contact with the surface of PET; (ii) enzyme–substrate complex formation: a PET chain must enter into the active site of the enzyme and adopt a pose ready for the hydrolysis reaction to take place; (iii) catalytic action: the PET hydrolase catalyzes the hydrolysis reaction by cleaving the ester bond(s) in the polymer chain; and (iv) product release: after the reaction, the products (e.g., shorter PET chains, BHET, MHET, TPA, and EG) must be released from the active site of the enzyme, allowing the enzyme to be free for additional catalytic cycles.

Insoluble substrates like PET present unique challenges for enzymes. Unlike soluble substrates that easily dissolve in water and are accessible to enzymes, insoluble substrates remain solid and often possess complex structures that enzymes must navigate. The enzymatic hydrolysis of PET primarily involves surface erosion, where the outer polymer layer is degraded to expose inner material. Due to the inability of water and enzyme molecules to penetrate the polymer's core, only a limited number of ester bonds are accessible for enzymatic action. Additionally, interfacial enzymes, such as PET hydrolases, must overcome attractive forces within the substrate matrix to form a productive enzyme–substrate complex.

Based on the PET hydrolase catalytic cycle, one can focus on one or more of the four major steps to increase its efficiency. Most approaches so far emphasize optimizing the second and third steps, specifically the binding of PET in the active site and the catalytic reaction. It is important to consider the material properties of PET, a semi-crystalline thermoplastic with linear polymer strands forming both amorphous and crystalline regions (Figure 2). The mobility of the PET chains is temperature-dependent, transitioning from rigidity below the **glass transition temperature** (T_g) to flexibility above it. The T_g differs between the amorphous and rigid regions, as well as between bulk PET and the surface, due to the plasticization effect of water [19–22]. Increased flexibility allows better access to ester bonds, enhancing enzymatic turnover [23]. Optimal PET biodegradation therefore occurs at 68–72°C [5,19,22,24,25], necessitating high thermostability in PET hydrolases. The thermostability of enzymes can be improved by introducing covalent disulfide bridges, which resulted in increases in melting temperature (T_m) of 20–30°C for various PET-degrading enzymes [26–28]. Techniques like directed evolution, machine learning (ML), and artificial intelligence (AI) have also been used to create thermostable enzyme variants, such

Glossary

Atomic force microscopy-single-molecule force spectroscopy (AFM-SMFS): measures forces and interactions at the level of individual molecules using an AFM tip to apply force to a single molecule; provides information on unfolding or binding interactions.
Carbohydrate-binding domain (CBM): a specific structural region found in certain proteins that enables them to bind carbohydrates.
Crystallinity (X_c): level of structural order within a solid; impacts properties such as hardness, density, transparency, and diffusion.
Fluorescence recovery after photobleaching (FRAP) microscopy: quantitative imaging technique for studying the dynamics of fluorescently labeled molecules in tissue or cells; a specific region is photobleached and the recovery of fluorescence is monitored to analyze molecular diffusion.
Glass transition temperature (T_g): gradual and reversible change in amorphous material domains from a hard, brittle 'glassy' state to a viscous or rubbery state as temperature increases.
Hamiltonian replica exchange molecular dynamics (HREMD): computational technique to enhance sampling in molecular dynamics simulations; multiple system replicas are created with different Hamiltonians and exchanged periodically.
Heterogeneous catalysis: process where the catalyst is in a different phase from the reactants.
Inverse Michaelis–Menten: a reciprocal form of the conventional Michaelis–Menten kinetics, where the concentration of the enzyme exceeds that of the substrate.
Isothermal titration calorimetry (ITC): measures heat changes during a chemical reaction or binding event; determination of the thermodynamics of interactions such as binding constants and enthalpy changes.
Langmuir isotherms: describe the adsorption of molecules onto a solid surface as a function of pressure, assuming uniform binding sites, where an occupied site cannot accommodate another molecule.
Molecular docking: prediction of the preferred orientation of one molecule when binding to another; binding affinity is estimated using a scoring function.

as HotPETase and DuraPETase, which are both derived from the *Is*PETase [29,30]. Using a structure-based ML approach, FAST-PETase was developed [31]. Meanwhile, a combination of **molecular dynamics (MD) simulations** and ML facilitated the prediction of variants of *T. fusca* Cutinase 2 (TfC2) with enhanced thermostability [32], which, as the WT, already has a very high melting temperature (T_m) of 92.8°C.

While elevated temperatures are needed for efficient PET entry into the active site, increased polymer mobility enables recrystallization – a process known as physical aging – and a higher degree of **crystallinity** (X_c) restricts PET access, reducing turnover [22,33,34]. This physical aging begins above 72°C for amorphous PET in an aqueous environment [5]. Therefore, developing highly efficient enzymes that can outperform this competing physical aging process is essential [20,21], a challenge addressed through PET hydrolase engineering. To this end, many studies investigated the interactions between PET and amino acids near the active site, examining crystal structures of enzymes with PET analogs [6,35–41], as well as structures based on **molecular docking** [5,40,42–44], often followed by short MD simulations [6,45–49]. Studies have replaced sterically demanding amino acids with smaller ones to widen the binding cleft of PET-degrading enzymes, enhancing activity due to improved accessibility [43,50–52]. However, such substitutions might lead to the loss of specific interactions with PET, weakening binding. In fact, in one study, narrowing the binding site and introducing amino acids with stronger PET interactions has led to increased activity [49]. Increased aromaticity [50] and hydrophobicity [52,53] near the active site also positively influence activity. A conserved tryptophan, known as 'wobbling' tryptophan, located at one end of the catalytic binding cleft, enhances PET binding through π–π interactions with the benzene ring and improves product release [40,54].

To gain insights into the mechanistic details of the catalytic reaction beyond the assumptions derived from crystal structures, **quantum mechanics/molecular mechanics (QM/MM)** simulations were conducted, with the first studies on enzymatic PET hydrolysis published in 2021 [55–57], followed by several other studies in subsequent years [58–61]. The mechanism consists of acylation, where the catalytic serine's nucleophilicity is increased by proton transfer from the histidine, allowing for an attack on the PET ester's carbonyl and the subsequent cleavage of the bond, and deacylation, where a water molecule attacks the acyl intermediate. Key mutations, such as the replacement of an isoleucine near the catalytic aspartate with alanine, resulted in a loss of activity, emphasizing the importance of nearby amino acids in stabilizing the catalytic aspartate [62]. A recent QM/MM study disclosed that the acylation process in LCC and PES-H1, along with their more active mutants LCC^{ICCG} and PES-H1^{FY}, involves two distinct conformations of the PET benzene ring that enhance π–π interactions with the 'wobbling' tryptophan residue [63]. For the high-activity variants LCC^{ICCG} and PES-H1^{FY}, a reduction of 2–5 kcal/mol in activation free energy was observed compared with their respective WT enzyme and partially explains their increased activity. Alternative to molecular simulations, AI also offers promising avenues for optimizing the active sites of PET hydrolases; for example, a recent study utilized a diffusion model combined with a neural network approach to design tailor-made enzymes, specifically generating novel serine hydrolases for the hydrolysis of PET [64].

Attempts were also made to increase enzymatic efficiency by addressing the first step of the catalytic cycle and modifying the interactions between PET hydrolases and the PET material. However, the collective findings from studies addressing these interactions indicate that this process is primarily nonspecific, which poses a challenge for enhancing enzymatic efficiency. In light of this, no explicit PET recognition site has been identified so far, prompting efforts to modify PET surface characteristics or fuse enzymes with binding domains to enhance adsorption [65]. For

Molecular dynamics (MD) simulations: computational method that models the motion of atoms and molecules over time, enabling the study of particle interactions in a defined system based on classical physics.
PET hydrolases: enzymes that catalyze the breakdown of PET by hydrolyzing the ester bonds.
Polyethylene terephthalate (PET): the most common thermoplastic polymer of the polyester family; used for beverage bottles and food packaging, textiles, thermal insulation materials, among others.
Quantum mechanics/molecular mechanics (QM/MM): combines accurate QM calculations for reactive sites or complex interactions with faster classical MM calculations for the surrounding environment.
Quartz crystal microbalance with dissipation monitoring (QCM-D): measures mass changes and viscoelastic properties of thin films on a quartz crystal sensor by monitoring changes in frequency and energy dissipation during adsorption or reaction processes.
Sabatier principle: concept in heterogeneous catalysis; asserts that the interactions between catalyst and reactant should not be too strong or too weak for optimal catalysis.
Total internal reflection fluorescence (TIRF) microscopy: uses a special light wave to light up only the molecules very close to a glass surface, allowing detailed imaging of thin layers or molecules interacting with a thin surface of material.
Zeta potential: the electrical potential at the slipping plane of a particle in a liquid (i.e., at the interface separating mobile fluid from fluid attached to the particle surface). Higher zeta potential values suggest greater particle stability in suspension, while lower values indicate a tendency for aggregation.

Table 1. Michaelis constant K_m, inverse Michaelis constant $^{inv}K_m$, and turnover rate k_{cat} of relevant PET hydrolases for amorphous and crystalline PET substrates

Enzyme	T [°C]	Amorphous PET substrate			Crystalline PET substrate		
		K_m [gL^{-1}]	$^{inv}K_m$ [μM]	k_{cat} [s^{-1}]	K_m [gL^{-1}]	$^{inv}K_m$ [μM]	k_{cat} [s^{-1}]
PES-H1^{FY}[8]	70	0.391	0.892	–	–	–	–
LCC [9]	50	–	–	–	1.8	0.086	0.29
LCC [10]	40	0.42	–	0.20	–	–	–
LCC ^{ICCG}[11]	60	–	–	–	2.9	–	0.6 (calculated)
LCC ^{ICCG}[8]	70	0.215	0.365	–	–	–	–
HiC [12]	50	–	–	–	0.27	0.043	0.088
HiC [12]	60	–	–	–	0.26	0.28	0.043
HiC [13]	50	2.655–3.852	5.81–8.27	0.0294–0.0843	2.458–2.683	1.54–5.22	0.0076–0.0107
TfC [12]	50	–	–	–	1.2	0.026	0.015
TfC [12]	60	–	–	–	0.68	0.20	0.052
TfC [9]	50	–	–	–	1	0.077	0.04
HotPETase [14]	–	3.41	0.79	0.13	3.26	0.59	0.13
*Is*PETase [12] (W159H/S238F)	40	–	–	–	4.9	0.039	0.52
*Is*PETase [12] (W159H/S238F)	50	–	–	–	0.24	–	0.69
*Is*PETase [15] (WT)	30	697	0.235	1.5	54	2.162	0.8
*Is*PETase [15] (WT)	40	87	0.309	0.5	26	2.037	1.7
*Is*PETase [15] (W159H/S238F)	30	302	2.690	0.5	479	1.303	0.5
*Is*PETase [15] (W159H/S238F)	40	141	0.527	0.5	95	1.874	1.2

example, **carbohydrate-binding domains (CBMs)**, known for efficiently binding polymers like synthetic plastics [66,67], have been fused terminally with PET-degrading enzymes [68–73]. These studies demonstrated that the impact of CBM fusion on activity depends on various parameters such as the catalytic domain, linker type, substrate type, and substrate load. The fusion of small anchor peptides to HotPETase has yielded similar results as with CBMs [14]. Additionally, fusing hydrophobins or adding them as free molecules enhances PET degradation by PET hydrolases [74–76]. Hydrophobins are small glycoproteins that modify the surface properties of hydrophobic substrates like PET, increasing their hydrophilicity and facilitating enzyme adsorption from the aqueous phase. This improved binding raises the local concentration of the enzyme on the substrate surface, enhances wettability, and promotes hydrolytic breakdown of PET [74–78]. An innovative approach for PET degradation involved codisplaying *Is*PETase and a hydrophobin on yeast, significantly increasing the degradation of highly crystalline PET compared with purified *Is*PETase [79]. Surfactants serve a similar function as hydrophobins, with their hydrophobic part binding to PET, while the charged part mediates contact with the enzyme, as demonstrated for *Is*PETase [80] and TfC2 [81].

In other studies the surface charge of the enzymes was directly addressed. For instance, Sagong *et al.* identified a positive effect by introducing negative charges in surface regions away from the catalytic center, while substitutions with negatively charged amino acids near the catalytic center resulted in reduced activity [82]. Jäckering *et al.* found that even substitutions involving only polar residues, rather than charged ones, on the protein surface far from the active site of PES-H1 significantly reduced its activity [8]. Thomsen *et al.* observed crater formation on the PET surface during its degradation with PES-H1, attributing this to PES-H1's low affinity for PET with high

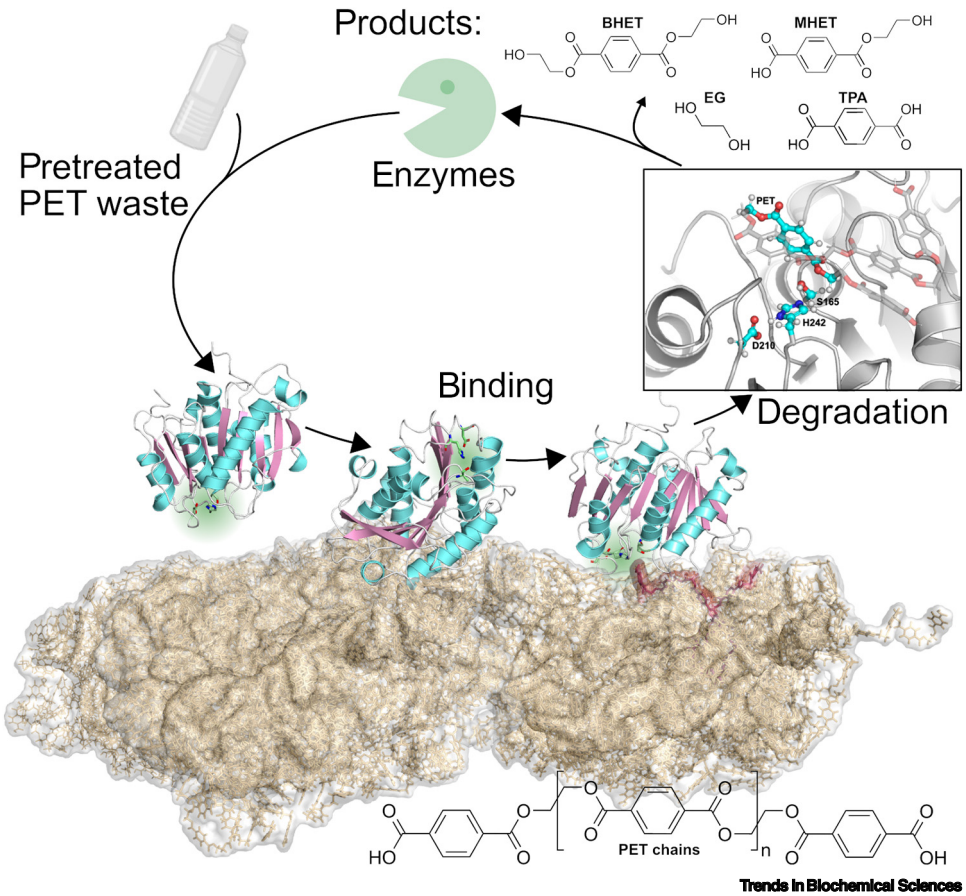

Figure 1. Schematic process of enzymatic plastic degradation. The polyethylene terephthalate (PET) waste is first pretreated, including micronization and amorphization, to facilitate the enzymatic hydrolysis process. The PET hydrolases (with the active site highlighted in green) then bind to the amorphous PET plastic polymers. One of the PET chains enters the active site, which contains the catalytic triad residues Ser, His, and Asp [shown here for leaf compost cutinase (LCC), Protein Data Bank 4EB0] [3], where the ester bonds are hydrolyzed. The PET chains are first degraded into shorter fragments, and the final products are the monomers bis(2-hydroxyethyl) terephthalate (BHET), mono(2-hydroxyethyl) terephthalate (MHET), terephthalic acid (TPA), and ethylene glycol (EG). After isolating the monomers and the enzymes, the enzymes can be reused for further plastic degradation.

crystallinity in combination with the enzyme's negative surface charge [83]. As degradation increases the number of negatively charged carboxylic groups on the PET surface, it becomes more negative, repelling PES-H1 and resulting in crater formation rather than uniform degradation. These observations are supported by different studies that indicated a positive impact of a more neutral, hydrophobic enzyme surface on enzymatic activity [84–86]. However, enhancing PET adsorption does not always translate to increased PET hydrolase activity; in fact, improved activity can sometimes be achieved by reducing adsorption, as seen in LCC, where a decreased binding affinity arises from cationic surfactants [9]. This observation aligns with the **Sabatier principle**, which posits that there is an optimal binding affinity for achieving the most effective enzymatic activity. If the binding is too strong, it can hinder the release of the reactants after catalysis took place, reducing the catalytic turnover; conversely, if the binding is too weak, the catalyst may not hold the reactants long enough for the reaction to occur. Thus, an intermediate binding strength is ideal, as it maximizes catalytic efficiency by enabling enzymes to stabilize transition states without obstructing product release [87].

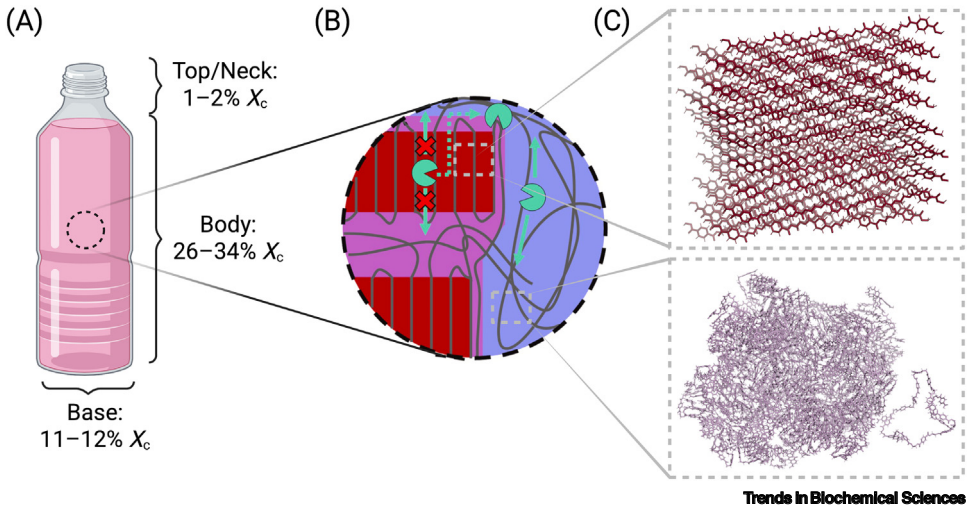

Figure 2. Crystalline and amorphous polyethylene terephthalate (PET). (A) The degree of crystallinity (X_c) varies in different regions of a PET bottle. (B) Zooming into the PET materials shows a lamellar structure consisting of crystalline (deep red) and amorphous layers (lilac). Enzymatic attack is only possible in the amorphous regions where individual PET chains are accessible by the active sites of PET hydrolases (green icons). (C) The molecular structures of crystalline (top) and amorphous (bottom) PET show their differences in order. The figures in panels (A) and (B) are reproduced and adapted with permission from [18].

Since the optimal binding between the PET surface and PET hydrolases has not yet been established, and it remains unclear why surface mutations in the enzyme, distant from the active site, can significantly reduce activity [8], it is essential to better understand the interplay between PET hydrolase binding and the characteristics of both the enzyme and the PET surface. Consequently, the remainder of this review focuses on this aspect, discussing various experimental and simulation techniques that can be employed to further investigate these interactions.

Experimental approaches for studying PET surface–PET hydrolase interactions

Experimental methods are essential for elucidating the interactions between PET surfaces and hydrolases, providing direct observations and quantitative data for analyzing enzyme binding and activity. The techniques discussed in the following section are biophysical methods commonly employed to investigate interface-related problems, enabling the determination of binding affinities, surface interactions, protein mobility, and the kinetics of the process.

Langmuir isotherms are commonly used to determine protein binding to insoluble substrates. This model describes the adsorption of protein molecules onto a homogeneous solid substrate surface with identical binding sites, assuming independent protein binding, monolayer formation, and reversible binding. Despite their simplicity, the Langmuir isotherms are often overlooked in PET hydrolase studies. Nonetheless, in one study the method was applied to measure the interactions between semi-crystalline PET powder and three different PET hydrolases, two cutinases (TfC and HiC from *Humicola insolens*) and a variant of the *Is*PETase, under conditions of both enzyme and substrate excess [65]. The binding process was reasonably described by a Langmuir isotherm, indicating a strong affinity for the PET substrate, with dissociation constants consistently below 150 nM. The saturated substrate coverage for all three enzymes roughly corresponded to a monolayer on the PET surface. No specific ligand binding contributions in the active site were identified, suggesting that adsorption is predominantly driven by nonspecific interactions, unlike enzymes naturally evolved to degrade insoluble polymers. However, a correlation was observed between the progression of enzymatic hydrolysis and increased binding

capacity, likely due to surface modifications of the PET polymer over time. In another study, Langmuir isotherms identified that fusing CBMs to a variant of LCC improved the affinity of the enzyme to PET [72]. Binding isotherms, along with **zeta potential** measurements that quantify the electrical charge on the surface of particles such as proteins in a liquid, helped explain the differences in activity as a function of salt concentration for several HiC homologs.

An **inverse Michaelis–Menten** approach has been used to assess the kinetics of PET hydrolases and their interaction with the PET surface. Besides the kinetic parameters, this approach provides the number of attack sites on the PET surface. Specifically, one kinetic data set is collected using the conventional method with the substrate in excess, while another is collected in an inverse concentration regime with enzyme in excess (Figure 3A) [9]. This approach has been applied using either PET powder or film of varying crystallinity, yielding substrate affinity, turnover rate, catalytic efficiency, and the ability to identify attack sites on PET, thereby facilitating the identification of rate-limiting steps [9,15,88–91]. For example, it was used to compare an engineered PET hydrolase, TurboPETase, with other PET hydrolases. It was suggested that TurboPETase's enhanced depolymerization performance may, at least in part, be due to its improved ability to target a broader range of specific attack sites that can be hydrolyzed [88]. The inverse Michaelis–Menten approach was also used to

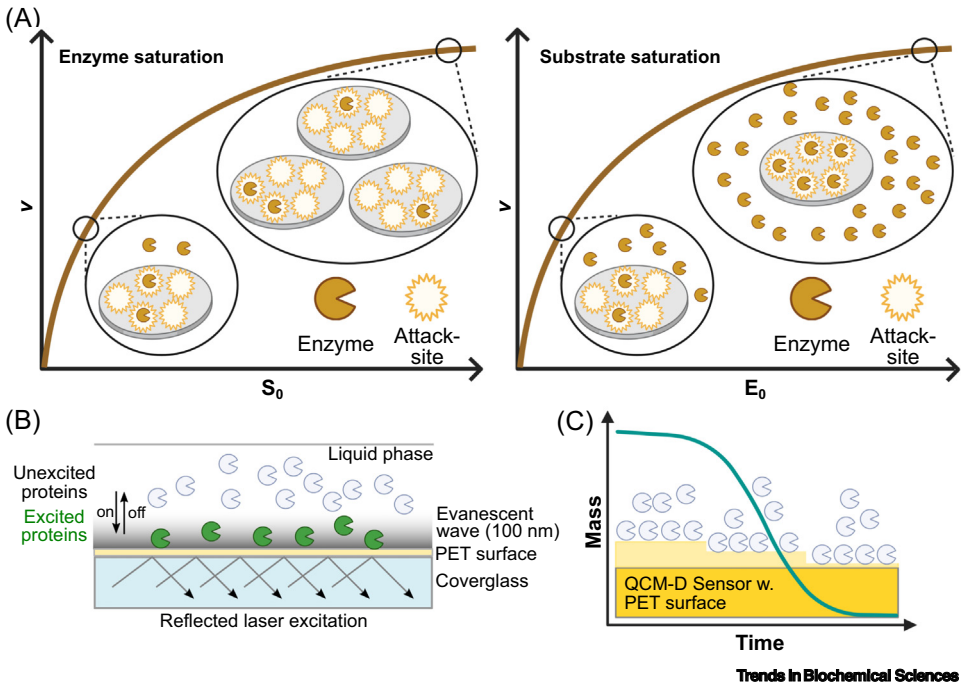

Figure 3. Principles behind selected experimental methods used for characterizing polyethylene terephthalate (PET) hydrolase interactions with PET surfaces and their hydrolysis of insoluble PET. (A) Analysis of heterogeneous enzyme catalysis can be approached through two alternative methods: enzyme saturation (left), that is, the conventional Michaelis–Menten analysis with initial rate (v) plotted against total substrate concentration (S_0), and substrate saturation (right), that is, an inverse Michaelis–Menten analysis with initial rate (v) plotted against total enzyme concentration (E_0). The density of attack sites on the insoluble substrate can be determined based on these analyses [96]. (B) The principle behind total internal reflection fluorescence (TIRF) microscopy used for analyzing enzyme–PET interactions. Fluorophore-labeled PET hydrolases in solution are placed on a coverglass with a thin PET film cast on it. Proteins close enough to the surface ($<$ 100 nm) will be excited and hence give a signal, which can be measured. These data can be used to determine on and off rates. (C) Example of quartz crystal microbalance with dissipation monitoring (QCM-D) in relation to PET hydrolase activity. The degradation of the PET film on the sensor surface by PET hydrolases is followed by the change in mass over time.

study the effect of the surfactant cetylmethylammonium bromide (CTAB) on the enzymatic activity and strength of enzyme–PET interactions of LCC and TfC [9]. CTAB consistently reduced the interaction strength, while its effect on enzymatic turnover exhibited a strong biphasic response. Initially, increasing the concentration of CTAB enhanced turnover, but beyond a certain point, the turnover was suppressed. This correlation reflects the Sabatier principle [9].

Isothermal titration calorimetry (ITC), combined with thermokinetic models, was employed to conduct a detailed analysis of the degradation process of PET nanoparticles by TfC2 [92]. An inverse Michaelis–Menten-based model was used for the data analysis. The results determined that about 95% of the heat produced during PET degradation can be attributed to the heat of reaction, while only about 5% was due to the heat of adsorption.

The effect of surface mutations on a PET hydrolase, PET2, identified from a metagenome library, was investigated using **total internal reflection fluorescence (TIRF) microscopy**. This technique enables single-molecule imaging, allowing for the tracking of binding rate constants (Figure 3B). The most active mutant exhibited an increased binding rate constant, which was suggested to explain its higher activity compared with the WT enzyme [37]. In another study, TIRF microscopy was combined with **fluorescence recovery after photobleaching (FRAP)** microscopy to examine how two green fluorescence protein (GFP) labeled PET hydrolases, LCC and PES-H1 (aka PHL7), and their CBM fusion variants attach and detach from a PET surface. TIRF microscopy was optimized for measuring the on and off rates of the enzymes, while FRAP microscopy was used to assess the dynamic movement rates of proteins across the PET surface. The study showed that adsorption and desorption dominate over lateral diffusion [93]. Similarly, single-molecule binding dynamics of quantum dot-labeled *Is*PETase were studied using TIRF microscopy. Specifically, the landing rate and the binding duration were measured. The binding durations were well described by a biexponential model, featuring a fast population interpreted as active binding events and a slow population representing nonspecific binding interactions [94]. Additionally, a simplified form of TIRF microscopy was utilized to study enzyme density and distribution on the PET surface, providing insights into the protein concentration-dependent activity reduction of *Is*PETase [95].

The **quartz crystal microbalance with dissipation monitoring (QCM-D)** is a method that allows for real-time monitoring of PET hydrolysis, enabling the determination of depolymerization kinetics. This was demonstrated for TfC2 and its mutants, where QCM-D was used to analyze the degradation kinetics of PET spun-coated onto a gold sensor (Figure 3C), which revealed two distinct phases: an 'initial hydrolysis phase' and a 'fast hydrolysis phase' [97]. Furthermore, earlier research employed QCM to evaluate the effects of fusing binding proteins including CBMs to a PET hydrolase on the hydrolysis kinetics [69].

Thermal treatment of a WCCG variant of LCC was shown to enhance PET hydrolysis. To elucidate the underlying reasons, **atomic force microscopy-single-molecule force spectroscopy (AFM-SMFS)** was employed to assess enzyme adsorption to a PET surface [89]. This method uses a sharp AFM tip to apply controlled forces to a single molecule measuring the forces needed to unfold or detach it from a surface, providing detailed insights into molecular interactions, binding strengths, and conformational changes [98]. Untreated and thermally treated enzyme were applied to the AFM tip and approached a PET film. Thermally treated enzyme showed higher adhesion force than the untreated one. It was hypothesized that thermal treatment increases the hydrophobicity of the protein surface [89]. AFM-SMFS was also used to demonstrate that hydrophobic anchor peptides promote adhesive interactions between HotPETase fused with different anchor peptides and the PET surface [14].

We find it important to note that the outcome of all the experimental methods described depends on the properties of the PET substrate. The degree of crystallinity is crucial when assaying and comparing the activity of PET hydrolases on insoluble PET, with enzymatic activity increasing when the crystallinity decreases [18,23,73,83]. However, crystallinity is an overall estimate and does not reflect the specific properties of the PET surface where the PET hydrolases act. Some PET hydrolases create holes in the substrate, likely targeting amorphous areas of the substrate surface [83]. So far, no experimental framework has yet fully captured the relationship between PET surface morphology and PET hydrolase activity [99]. Single-molecule microscopy methods and QCM-D face challenges in preparing the PET surface, as PET is dissolved in an organic solvent before being cast onto a cover slip. This process results in a PET layer that is not directly comparable with insoluble PET substrates used in activity analyses. Furthermore, PET autofluorescence issues require pretreatment of the PET surface and extensive data processing [37,93].

Molecular simulations for studying PET surface–PET hydrolase interactions

Molecular simulations offer a promising complement to experimental approaches for understanding PET hydrolase interactions with PET surfaces. By allowing precise control over variables like surface morphology and molecular interactions, simulations can provide detailed insights into mechanistic relationships that are challenging to capture experimentally; however, they also come with their own challenges, which are discussed later. While the docking and QM/MM simulations provide crucial insights into the processes within the active site (discussed earlier), they are not able to explain how the enzymes adsorb on the PET material and how PET reaches the active site. These questions can be addressed by classical MD simulations where PET is modeled as a material in its amorphous, crystalline, or mixed amorphous/crystalline state (Figure 2) and the respective enzyme is placed above the material to monitor the adsorption process.

In the study by Sahihi *et al.*, the adsorption of LCC^{ICCG} on amorphous PET consisting of PET-9mer chains at 65°C was simulated [100]. The enzyme was always positioned such that the active site faced the PET material and was only about 5 Å away. Consequently, the enzyme always bound with the same area to the PET surface, and this interaction occurred rapidly and was mediated by hydrophobic, hydrogen bond, and π–π interactions between PET chains and various amino acid residues of the cutinase enzyme. Notably, the presence of the enzyme aided in extracting a PET monomer into the water.

Jäckering *et al.* conducted a detailed analysis of PET hydrolase binding to amorphous PET at 30°C for LCC and PES-H1, starting from random orientations at least 10 Å away from a bulk of PET-9mers [8]. Their findings indicated that initial adsorption is predominantly nonspecific, occurring in both proximal and distal regions relative to the enzymes' active site, with minimal protein reorientation taking place on the PET surface, even when extending simulations to 2 μs (Figure 4A). Interaction energy analysis disclosed that mainly polar and hydrophobic interactions drive adsorption, while repulsion occurs with negatively charged residues, which are more prevalent in PES-H1 compared with LCC (Figure 4B). To further explore the role of specific amino acids in PET interactions, surface residues were mutated to weaken PET binding, primarily replacing positively charged and polar residues with negatively charged ones or alanine (Figure 4C,D). *In silico* simulations of the resulting triple mutants guided the selection for *in vitro* testing using the inverse Michaelis–Menten approach, but the LCC mutant could not be expressed despite mutations being distant from the active site. Meanwhile, the PES-H1 T11V/S13A/S14A mutant exhibited significantly reduced PET degradation activity. This observation aligns with the Sabatier principle, indicating that the PES-H1 triple mutant may have weakened interactions too much for optimal catalysis [8]. These results highlight the importance of

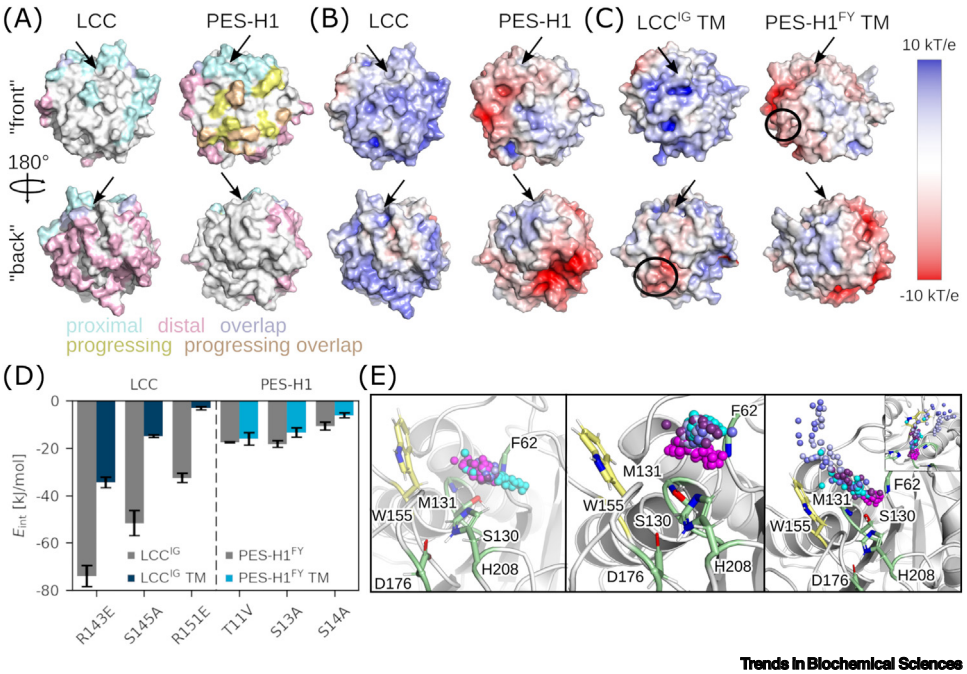

Figure 4. Molecular dynamics (MD) analysis of polyethylene terephthalate (PET) hydrolase binding on amorphous PET. (A) Residues in contact with PET during the adsorption of leaf compost cutinase (LCC) [left, Protein Data Bank (PDB) 4EB0] [3] and polyester hydrolase I (PES-H1) (right, PDB 7CUV) [6] for at least 75% of the simulation time are colored blue and rose for proximal and distal sites, respectively, relative to the catalytic site (indicated by an arrow), with overlapping areas in purple. One PES-H1 simulation showed enzyme relocation from distal to proximal binding, highlighted in yellow. (B) Electrostatic potential surfaces (EPS) for LCC (left, net charge: +5) and PES-H1 (right, net charge: − 5) disclose that negatively charged areas in PES-H1 avoided PET. (C) EPS of the LCC^{IG} triple mutant (TM) and PES-H1^{FY} TM. Mutations are within the black circle and the catalytic site is indicated by an arrow. (D) MD interaction energies between PET and the mutation site residues show weaker binding for the TMs (blue) compared with parent enzymes (gray). *In vitro*, LCC^{IG} TM could not be expressed, while PES-H1^{FY} TM lost over 50% activity. (E) Analysis of PET entry into the active site identified three dominant pathways for PES-H1 (with key residues like the catalytic triad S130/D176/H2028 and the 'wobbly' W155 highlighted); pathways are shown as spheres (reflecting PET ester carbons that are eventually productively bound) on the enzyme structure, with sphere color indicating entry progress from cyan to magenta. Plots reproduced with permission from Ref. [8].

understanding enzymatic adsorption to PET, as even minor distant mutations can greatly affect protein stability and activity through alterations in PET adsorption dynamics.

Since Jäckering *et al.* did not observe PET-9mer penetration into the binding cleft during their 2 μs MD simulations at 30°C, this indicates an energy barrier impeding PET entry into the active site. To investigate this further, they employed **Hamiltonian replica exchange molecular dynamics (HREMD)**, modifying the energy function of PET to enhance its mobility at higher replicas, thereby allowing exploration of PET entry for the first time in LCC and PES-H1 [8]. This approach confirmed the energy barrier's presence, attributed to intramolecular PET–PET interactions needing resolution before PET could insert into the binding cleft, along with intermolecular PET–residue interactions hindering productive binding poses. It was found that raising the temperature to 70°C could overcome the obstructive PET–PET interactions, partly explaining why enzymatic PET degradation is generally more efficient at higher temperatures (Table 1). Free energy analysis and principal component analysis of the HREMD data identified three main PET entry pathways (Figure 4E) and unfavorable PET–residue interactions that could be mitigated by mutations T211G in LCC and S68A in PES-H1, as confirmed by *in vitro* tests.

Paiva *et al.* investigated the adsorptions process of the *Is*PETase on amorphous and crystalline PET [101]. MD simulations at 30°C of the PET–*Is*PETase systems identified a preference for the amorphous PET substrate, which correlates with the established experimental data (Table 1). The computational models developed by Paiva *et al.* associate this tendency with a substantially higher PET–*Is*PETase contact area, a better PET chain accessibility, and a beneficial organization of the catalytic triad in the case of the amorphous PET substrate, which is evident from inspecting the molecular structures of crystalline and amorphous PET shown in Figure 2.

The study by Chen *et al.* combined computational and experimental methods to obtain a complete catalytic pathway for the enzymatic degradation of PET by the *Is*PETase and with that providing additional information on the functional properties of PET hydrolases [102]. This includes enzyme binding, PET fragment capture, conformational refinement, attainment of the final pre-cleavage conformation, and ester bond cleavage. The conducted MD simulations allowed for the sampling cleavable PET conformations and provided an explanation for the experimentally observed enzyme inactivation in the form of conformational fluctuations in the catalytic loop. While for *Is*PETase these fluctuations may increase the PET capture capability at the cost of enzyme stability, a comparison with its more thermostable mutant, the HotPETase, led to the conclusion that this activity–stability trade-off can be overcome through directed evolution.

An MD study focusing on crystalline PET explored the adsorption of CBMs as promising candidates for fusion with PET hydrolases to enhance enzyme activity by increasing substrate affinity [66]. This study started with an *in vitro* analysis of eight CBMs for their PET binding affinity. A fast and reliable PET surface affinity assay was developed for semi-quantitative analysis of protein–PET interactions, which identified a *Bacillus anthracis* CBM from family 2 (*Ba*CBM2) as a high-affinity PET binder. MD simulations indicated that surface-exposed aromatic triads in *Ba*CBM2 interacted with PET through π-stacking – which is less significant for binding to amorphous PET [8] – and polar interactions. These findings were supported by tryptophan fluorescence quenching experiments, which allowed for the determination of a dissociation constant for *Ba*CBM2 ($K_d = 25.4\ \mu g\ L^{-1}$). The balance of hydrophobic to polar interactions at the CBM–PET interface differentiated high-affinity binders, with *Ba*CBM2 demonstrating an optimal ratio, from CBMs with lower affinity [66].

Concluding remarks

The remarkable similarity between man-made plastics and natural polymers allows certain enzymes, such as cutinases and other polyesterases, to effectively degrade plastics like PET. However, the WT forms of these enzymes often lack the efficiency required for practical industrial applications. To rationally enhance their performance, a thorough understanding of the heterogeneous catalytic process is essential, beginning with the adsorption of enzymes onto insoluble PET and culminating in product release. While many studies concentrate on elucidating the processes within the active sites of PET hydrolases, we advocate for increased research into the interactions between these enzymes and the PET material, both at the onset of degradation and during the process, particularly as PET undergoes structural and physicochemical changes due to shortened chains. As highlighted in this review, a diverse array of experimental and simulation techniques is available to advance our understanding in this area. We encourage the integration of these methods to achieve a more comprehensive analysis. Ultimately, by gaining deeper insights into the surface processes involved in PET degradation, we can strategically modify PET hydrolase surfaces to achieve the optimal binding conditions described by the Sabatier principle, thereby enhancing their catalytic efficiency and paving the way for effective solutions in plastic waste management (see Outstanding questions).

Outstanding questions

Mechanisms of action:

- What are the precise molecular mechanisms through which PET hydrolases interact with and degrade PET?
- How does the surface morphology influence these mechanisms?

Enzyme adsorption:

- Why has the adsorption of PET hydrolases to PET surfaces received less attention?
- What specific factors determine the efficiency of this adsorption and its implications for enzyme activity?

Engineering strategies:

- What are the most effective strategies for enhancing the catalytic efficiency of PET hydrolases?
- How can a better understanding of the interactions between PET material and PET hydrolases inform targeted engineering?

How can we encourage the field to integrate different simulation and experimental methods to achieve a more comprehensive approach to the study and design of PET hydrolases?

Acknowledgments

A.J. received funding from the German Federal Environmental Foundation (Deutsche Bundesstiftung Umwelt) through a PhD fellowship, while M.S.M. was supported by the Independent Research Fund Denmark (grant no. 1032-00273B).

Declaration of interests

The authors declare no competing interests.

References

1. Müller, R.J. *et al.* (2005) Enzymatic degradation of poly(ethylene terephthalate): rapid hydrolyse using a hydrolase from *T. fusca*. *Macromol. Rapid Commun.* 26, 1400–1405
2. Buchholz, P.C.F. *et al.* (2022) Plastics degradation by hydrolytic enzymes: the plastics-active enzymes database—PAZy. *Proteins* 90, 1443–1456
3. Sulaiman, S. *et al.* (2014) Crystal structure and thermodynamic and kinetic stability of metagenome-derived LC-cutinase. *Biochemistry* 53, 1858–1869
4. Sonnendecker, C. *et al.* (2022) Low carbon footprint recycling of post-consumer PET plastic with a metagenomic polyester hydrolase. *ChemSusChem* 15, e202101062
5. Tournier, V. *et al.* (2020) An engineered PET depolymerase to break down and recycle plastic bottles. *Nature* 580, 216–219
6. Pfaff, L. *et al.* (2022) Multiple substrate binding mode-guided engineering of a thermophilic PET hydrolase. *ACS Catal.* 12, 9790–9800
7. Yoshida, S. *et al.* (2016) A bacterium that degrades and assimilates poly(ethylene terephthalate). *Science* 351, 1196–1199
8. Jäckering, A. *et al.* (2024) From bulk to binding: decoding the entry of PET into hydrolase binding pockets. *JACS Au* 4, 4000–4012
9. Bååth, J.A. *et al.* (2022) Sabatier principle for rationalizing enzymatic hydrolysis of a synthetic polyester. *JACS Au* 2, 1223–1231
10. Robles-Martín, A. *et al.* (2023) Sub-micro-and nano-sized polyethylene terephthalate deconstruction with engineered protein nanopores. *Nat. Catal.* 6, 1174–1185
11. Jia, Q. *et al.* (2024) Enhanced degradation of post-consumer polyethylene terephthalate (PET) wastes by fusion cutinase: effects of anchor and linker peptides. *Process Biochem.* 145, 1–12
12. Bååth, J.A. *et al.* (2021) Comparative biochemistry of four polyester (PET) hydrolases. *ChemBioChem* 22, 1627–1637
13. Kamal, S. *et al.* (2025) Combined adsorption and Michaelis–Menten approach reveals predominant enzymatic depolymerization of crystalline poly (ethylene terephthalate) by *Humicola insolens* cutinase in the solution phase. *ACS Sustain. Chem. Eng.* 13, 2401–2410
14. Wang, Y. *et al.* (2025) Fusion of hydrophobic anchor peptides promotes the hydrolytic activity of PETase but not the extent of PET depolymerization. *ChemCatChem* 17, e202401252
15. Erickson, E. *et al.* (2022) Comparative performance of PETase as a function of reaction conditions, substrate properties, and product accumulation. *ChemSusChem* 15, e202101932
16. Arnal, G. *et al.* (2023) Assessment of four engineered PET degrading enzymes considering large-scale industrial applications. *ACS Catal.* 13, 13156–13166
17. Uekert, T. *et al.* (2022) Life cycle assessment of enzymatic poly (ethylene terephthalate) recycling. *Green Chem.* 24, 6531–6543
18. Thomsen, T.B. *et al.* (2023) Significance of poly(ethylene terephthalate)(PET) substrate crystallinity on enzymatic degradation. *New Biotechnol.* 78, 162–172
19. Tarazona, N.A. *et al.* (2022) Rapid depolymerization of poly(ethylene terephthalate) thin films by a dual-enzyme system and its impact on material properties. *Chem. Catal.* 2, 3573–3589
20. Taniguchi, I. *et al.* (2019) Biodegradation of PET: current status and application aspects. *ACS Catal.* 9, 4089–4105
21. Wei, R. *et al.* (2019) Biocatalytic degradation efficiency of post-consumer polyethylene terephthalate packaging determined by their polymer microstructures. *Adv. Sci.* 6, 1900491
22. Thomsen, T.B. *et al.* (2022) Influence of substrate crystallinity and glass transition temperature on enzymatic degradation of polyethylene terephthalate (PET). *New Biotechnol.* 69, 28–35
23. Schubert, S.W. *et al.* (2024) Relationships of crystallinity and reaction rates for enzymatic degradation of poly(ethylene terephthalate), PET. *ChemSusChem* 17, e202301752
24. Wei, R. *et al.* (2022) Mechanism-based design of efficient PET hydrolases. *ACS Catal.* 12, 3382–3396
25. Wellen, R. and Rabello, M. (2005) The kinetics of isothermal cold crystallization and tensile properties of poly(ethylene terephthalate). *J. Mat. Sci.* 40, 6099–6104
26. Oda, M. *et al.* (2018) Enzymatic hydrolysis of PET: functional roles of three Ca^{2+} ions bound to a cutinase-like enzyme, cut190*, and its engineering for improved activity. *Appl. Microbiol. Biotechnol.* 102, 10067–10077
27. Zhong-Johnson, E.Z.L. *et al.* (2021) An absorbance method for analysis of enzymatic degradation kinetics of poly(ethylene terephthalate) films. *Sci. Rep.* 11, 928
28. Brott, S. *et al.* (2022) Engineering and evaluation of thermostable *Is*PETase variants for PET degradation. *Eng. Life Sci.* 22, 192–203
29. Bell, E.L. *et al.* (2022) Directed evolution of an efficient and thermostable PET depolymerase. *Nat. Catal.* 5, 673–681
30. Cui, Y. *et al.* (2021) Computational redesign of a PETase for plastic biodegradation under ambient condition by the grape strategy. *ACS Catal.* 11, 1340–1350
31. Lu, H. *et al.* (2022) Machine learning-aided engineering of hydrolases for PET depolymerization. *Nature* 604, 662–667
32. Li, Q. *et al.* (2022) Computational design of a cutinase for plastic biodegradation by mining molecular dynamics simulations trajectories. *Comput. Struct. Biotechnol. J.* 20, 459–470
33. Sun, F. *et al.* (2022) Molecular-level investigation of plasticization of polyethylene terephthalate (PET) in supercritical carbon dioxide via molecular dynamics simulation. *R. Soc. Open Sci.* 9, 220606
34. Panowicz, R. *et al.* (2021) Properties of polyethylene terephthalate (PET) after thermo-oxidative aging. *Materials* 14, 3833
35. Richter, P.K. *et al.* (2023) Structure and function of the metagenomic plastic-degrading polyester hydrolase PHL7 bound to its product. *Nat. Commun.* 14, 1905
36. Zeng, W. *et al.* (2022) Substrate-binding mode of a thermophilic PET hydrolase and engineering the enzyme to enhance the hydrolytic efficacy. *ACS Catal.* 12, 3033–3040
37. Nakamura, A. *et al.* (2021) Positive charge introduction on the surface of thermostabilized PET hydrolase facilitates PET binding and degradation. *ACS Catal.* 11, 8550–8564
38. Li, Z. *et al.* (2022) Structural insight and engineering of a plastic degrading hydrolase Ple629. *Biochem. Biophys. Res. Commun.* 626, 100–106
39. Yang, Y. *et al.* (2023) Complete bio-degradation of poly(butylene adipate-co-terephthalate) via engineered cutinases. *Nat. Commun.* 14, 1645
40. Han, X. *et al.* (2017) Structural insight into catalytic mechanism of PET hydrolase. *Nat. Commun.* 8, 2106
41. von Haugwitz, G. *et al.* (2022) Structural insights into (tere) phthalate-ester hydrolysis by a carboxylesterase and its role in promoting PET depolymerization. *ACS Catal.* 12, 15259–15270
42. Joo, S. *et al.* (2018) Structural insight into molecular mechanism of poly(ethylene terephthalate) degradation. *Nat. Commun.* 9, 382
43. Bollinger, A. *et al.* (2020) A novel polyester hydrolase from the marine bacterium *Pseudomonas aestusnigri* – structural and functional insights. *Front. Microbiol.* 11, 114
44. Kawabata, T. *et al.* (2017) Mutational analysis of cutinase-like enzyme, Cut190, based on the 3D docking structure with

model compounds of polyethylene terephthalate. *J. Biosci. Bioeng.* 124, 28–35
45. Fecker, T. *et al.* (2018) Active site flexibility as a hallmark for efficient PET degradation by *I. sakaiensis* PETase. *Biophys. J.* 114, 1302–1312
46. Charupanit, K. *et al.* (2022) In silico identification of potential sites for a plastic-degrading enzyme by a reverse screening through the protein sequence space and molecular dynamics simulations. *Molecules* 27, 3353
47. Pirillo, V. *et al.* (2021) An efficient protein evolution workflow for the improvement of bacterial PET hydrolyzing enzymes. *Int. J. Mol. Sci.* 23, 264
48. Aristizábal-Lanza, L. *et al.* (2022) Comparison of the enzymatic depolymerization of polyethylene terephthalate and Akestra™ using *Humicola insolens* cutinase. *Front. Chem. Eng.* 4, 1048744
49. Austin, H.P. *et al.* (2018) Characterization and engineering of a plastic-degrading aromatic polyesterase. *Proc. Natl. Acad. Sci. U. S. A.* 115, E4350–E4357
50. Liu, B. *et al.* (2018) Protein crystallography and site-direct mutagenesis analysis of the poly(ethylene terephthalate) hydrolase PETase from *Ideonella sakaiensis*. *ChemBioChem* 19, 1471–1475
51. Araújo, R. *et al.* (2007) Tailoring cutinase activity towards polyethylene terephthalate and polyamide 6,6 fibers. *J. Biotechnol.* 128, 849–857
52. Silva, C. *et al.* (2011) Engineered *Thermobifida fusca* cutinase with increased activity on polyester substrates. *Biotechnol. J.* 6, 1230–1239
53. Ma, Y. *et al.* (2018) Enhanced poly(ethylene terephthalate) hydrolase activity by protein engineering. *Engineering* 4, 888–893
54. Chen, C.C. *et al.* (2018) Structural studies reveal the molecular mechanism of PETase. *FEBS J.* 285, 3717–3723
55. Boneta, S. *et al.* (2021) QM/MM study of the enzymatic biodegradation mechanism of polyethylene terephthalate. *J. Chem. Inf. Model.* 61, 3041–3051
56. Feng, S. *et al.* (2021) *Is*PETase- and *Is*MHETase-catalyzed cascade degradation mechanism toward polyethylene terephthalate. *ACS Sustain. Chem. Eng.* 9, 9823–9832
57. Jerves, C. *et al.* (2021) Reaction mechanism of the PET degrading enzyme PETase studied with DFT/MM molecular dynamics simulations. *ACS Catal.* 11, 11626–11638
58. Zheng, M. *et al.* (2023) Enantioselectivity and origin of enhanced efficiency in polyethylene terephthalate hydrolases catalyzed depolymerization. *J. Hazard. Mater.* 452, 131295
59. Garca-Meseguer, R. *et al.* (2023) Insights into the enhancement of the poly(ethylene terephthalate) degradation by FAST-PETase from computational modeling. *J. Am. Chem. Soc.* 145, 19243–19255
60. Zheng, M. *et al.* (2022) Depolymerase-catalyzed polyethylene terephthalate hydrolysis: a unified mechanism revealed by quantum mechanics/molecular mechanics analysis. *i* 10, 7341–7348
61. Zheng, M. *et al.* (2023) Impacts of QM region sizes and conformation numbers on modelling enzyme reactions: a case study of polyethylene terephthalate hydrolase. *Phys. Chem. Chem. Phys.* 25, 31596–31603
62. Magalhães, R.P. *et al.* (2022) The critical role of Asp206 stabilizing residues on the catalytic mechanism of the *Ideonella sakaiensis* PETase. *Catal. Sci. Technol.* 12, 3474–3483
63. Jäckering, A. *et al.* (2024) Influence of wobbling tryptophan and mutations on PET degradation explored by QM/MM free energy calculations. *J. Chem. Inf. Model.* 64, 7544–7554
64. Lauko, A. *et al.* (2025) Computational design of serine hydrolases. *Science* 388, eadu2454
65. Badino, S.F. *et al.* (2021) Adsorption of enzymes with hydrolytic activity on polyethylene terephthalate. *Enzyme Microb. Tech.* 152, 109937
66. Weber, J. *et al.* (2019) Interaction of carbohydrate-binding modules with poly(ethylene terephthalate). *Appl. Microbiol. Biotechnol.* 103, 4801–4812
67. Rennison, A.P. *et al.* (2023) Protein-plastic interactions: the driving forces behind the high affinity of a carbohydrate-binding module for polyethylene terephthalate. *Sci. Total Environ.* 870, 161948
68. Zhang, Y. *et al.* (2013) Enhanced activity toward PET by site-directed mutagenesis of *Thermobifida fusca* cutinase–CBM fusion protein. *Carbohydr. Polym.* 97, 124–129
69. Ribitsch, D. *et al.* (2013) Fusion of binding domains to *Thermobifida cellulosilytica* cutinase to tune sorption characteristics and enhancing PET hydrolysis. *Biomacromolecules* 14, 1769–1776
70. Xue, R. *et al.* (2021) Fusion of chitin-binding domain from *Chitinolyticbacter meiyuanensis* SYBC-H1 to the leaf-branch compost cutinase for enhanced PET hydrolysis. *Front. Bioeng. Biotechnol.* 9, 762854
71. Dai, L. *et al.* (2021) Enhancing PET hydrolytic enzyme activity by fusion of the cellulose–binding domain of cellobiohydrolase I from *Trichoderma reesei*. *J. Biotechnol.* 334, 47–50
72. Graham, R. *et al.* (2022) The role of binding modules in enzymatic poly(ethylene terephthalate) hydrolysis at high-solids loadings. *Chem. Catal.* 2, 2644–2657
73. Rennison, A.P. *et al.* (2024) Comparative biochemistry of PET hydrolase-carbohydrate-binding module fusion enzymes on a variety of PET substrates. *Enzym. Microb. Technol.* 180, 110479
74. Espino-Rammer, L. *et al.* (2013) Two novel class II hydrophobins from *Trichoderma* spp. stimulate enzymatic hydrolysis of poly(ethylene terephthalate) when expressed as fusion proteins. *Appl. Environ. Microbiol.* 79, 4230–4238
75. Ribitsch, D. *et al.* (2015) Enhanced cutinase-catalyzed hydrolysis of polyethylene terephthalate by covalent fusion to hydrophobins. *Appl. Environ. Microbiol.* 81, 3586–3592
76. Puspitasari, N. *et al.* (2021) Fungal hydrophobin RolA enhanced PETase hydrolysis of polyethylene terephthalate. *Appl. Biochem. Biotechnol.* 193, 1284–1295
77. Wösten, H.A. and de Vocht, M.L. (2000) Hydrophobins, the fungal coat unravelled. *Biochim. Biophys. Acta* 1469, 79–86
78. Stanzione, I. *et al.* (2022) Innovative surface bio-functionalization by fungal hydrophobins and their engineered variants. *Front. Mol. Biosci.* 9, 959166
79. Chen, Z. *et al.* (2022) Biodegradation of highly crystallized poly (ethylene terephthalate) through cell surface codisplay of bacterial PETase and hydrophobin. *Nat. Commun.* 13, 7138
80. Furukawa, M. *et al.* (2018) Acceleration of enzymatic degradation of poly(ethylene terephthalate) by surface coating with anionic surfactants. *ChemSusChem* 11, 4018–4025
81. Furukawa, M. *et al.* (2019) Efficient degradation of poly(ethylene terephthalate) with *Thermobifida fusca* cutinase exhibiting improved catalytic activity generated using mutagenesis and additive-based approaches. *Sci. Rep.* 9, 16038
82. Sagong, H.Y. *et al.* (2021) Implications for the PET decomposition mechanism through similarity and dissimilarity between PETases from *Rhizobacter gummiphilus* and *Ideonella sakaiensis*. *J. Hazard. Mater.* 416, 126075
83. Thomsen, T.B. *et al.* (2023) Rate response of poly(ethylene terephthalate)-hydrolases to substrate crystallinity: basis for understanding the lag phase. *ChemSusChem* 16, e202300291
84. Thumarat, U. *et al.* (2012) Biochemical and genetic analysis of a cutinase-type polyesterase from a thermophilic *Thermobifida alba* AHK119. *Appl. Microbiol. Biotechnol.* 95, 419–430
85. Miyakawa, T. *et al.* (2015) Structural basis for the Ca^{2+}-enhanced thermostability and activity of PET-degrading cutinase-like enzyme from *Saccharomonospora viridis* AHK190. *Appl. Microbiol. Biotechnol.* 99, 4297–4307
86. Herrero Acero, E. *et al.* (2013) Surface engineering of a cutinase from *Thermobifida cellulosilytica* for improved polyester hydrolysis. *Biotechnol. Bioeng.* 110, 2581–2590
87. Kari, J. *et al.* (2018) Sabatier principle for interfacial (heterogeneous) enzyme catalysis. *ACS Catal.* 8, 11966–11972
88. Cui, Y. *et al.* (2024) Computational redesign of a hydrolase for nearly complete PET depolymerization at industrially relevant high-solids loading. *Nat. Commun.* 15, 1417
89. Akram, E. *et al.* (2024) On the temperature dependence of enzymatic degradation of poly(ethylene terephthalate). *Chin. J. Catal.* 60, 284–293
90. Zheng, Y. *et al.* (2024) Dynamic docking-assisted engineering of hydrolases for efficient PET depolymerization. *ACS Catal.* 14, 3627–3639

91. Thomsen, T.B. *et al.* (2024) Enzymatic degradation of poly(ethylene terephthalate)(PET): identifying the cause of the hypersensitive enzyme kinetic response to increased PET crystallinity. *Enzym. Microb. Technol.* 173, 110353
92. Vogel, K. *et al.* (2021) Enzymatic degradation of polyethylene terephthalate nanoplastics analyzed in real time by isothermal titration calorimetry. *Sci. Total Environ.* 773, 145111
93. Rennison, A.P. *et al.* (2024) Unveiling PET hydrolase surface dynamics through fluorescence microscopy. *ChemBioChem* 25, e202300661
94. Zhang, Y. and Hancock, W.O. (2024) Measuring PETase enzyme kinetics by single-molecule microscopy. *Biophys. J.* 123, 3669–3677
95. Zhong-Johnson, E.Z.L. *et al.* (2024) Analysis of poly(ethylene terephthalate) degradation kinetics of evolved *Is*petase variants using a surface crowding model. *J. Biol. Chem.* 300, 105783
96. Kari, J. *et al.* (2017) An inverse Michaelis–Menten approach for interfacial enzyme kinetics. *ACS Catal.* 7, 4904–4914
97. Meng, S. *et al.* (2023) Deep learning guided enzyme engineering of *Thermobifida fusca* cutinase for increased PET depolymerization. *Chin. J. Catal.* 50, 229–238
98. Tang, C. *et al.* (2018) Atomic force microscopy-based single molecule force spectroscopy for biological application. In *Atomic Force Microscopy in Molecular and Cell Biology* (Cai, J., ed.), pp. 29–40, Springer
99. Lippold, H. *et al.* (2022) Temporal and spatial evolution of enzymatic degradation of amorphous PET plastics. *NPJ Mat. Degrad.* 6, 93
100. Sahihi, M. *et al.* (2024) Probing enzymatic PET degradation: molecular dynamics analysis of cutinase adsorption and stability. *J. Chem. Inf. Model.* 64, 4112–4120
101. Paiva, P. *et al.* (2025) Atomistic adsorption of PETase onto large-scale PET 3D-models that mimic reality. *Phys. Chem. Chem. Phys.* 27, 2139–2150
102. Chen, S. *et al.* (2024) A mechanistic understanding of the activity-stability trade-off in PETase. *bioRxiv*, Published online June 9, 2025. https://doi.org/10.1101/2024.06.09.598049